AAPS PharmSciTech, Vol. 14, No. 1, March 2013 (© 2013)
DOI: 10.1208/s12249-013-9927-3

Research Article

Challenges in Detecting Magnesium Stearate Distribution in Tablets

Satu Lakio,[1,4] Balázs Vajna,[2] István Farkas,[2] Henri Salokangas,[3] György Marosi,[2] and Jouko Yliruusi[1]

Received 9 March 2012; accepted 12 January 2013; published online 2 February 2013

Abstract. Magnesium stearate (MS) is the most commonly used lubricant in pharmaceutical industry. During blending, MS particles form a thin layer on the surfaces of the excipient and drug particles prohibiting the bonding from forming between the particles. This hydrophobic layer decreases the tensile strength of tablets and prevents water from penetrating into the tablet restraining the disintegration and dissolution of the tablets. Although overlubrication of the powder mass during MS blending is a well-known problem, the lubricant distribution in tablets has traditionally been challenging to measure. There is currently no adequate analytical method to investigate this phenomenon. In this study, the distribution of MS in microcrystalline cellulose (MCC) tablets was investigated using three different blending scales. The crushing strength of the tablets was used as a secondary response, as its decrease is known to result from the overlubrication. In addition, coating of the MCC particles by MS in intact tablets was detected using Raman microscopic mapping. MS blending was more efficient in larger scales. Raman imaging was successfully applied to characterize MS distribution in MCC tablets despite low concentration of MS. The Raman method can provide highly valuable visual information about the proceeding of the MS blending process. However, the measuring set-up has to be carefully planned to establish reliable and reproducible results.

KEY WORDS: blending; lubricant; magnesium stearate; Raman spectroscopy; scale-up.

INTRODUCTION

Lubricant is added to tablet formulation to reduce die wall friction during compaction and ejection. They work by forming a layer between the particles and walls of the tableting die (1). In addition, dry lubricants enable compression with lower pressure, decrease the heat formation during tableting, and ensure the appropriate quality of tablets. Magnesium stearate (MS) is the most commonly used lubricant in pharmaceutical industry, since it lubricates the mass already in small amounts, and it has low friction coefficient and low shear strength (2). The applied MS concentration is usually 0.5–1% (*w*/*w*).

The effects of MS on the tablet properties have been studied since the 1950s. Its negative effects have also been reported since 1950s (3–7). One of the biggest disadvantages of MS is its tendency to dramatically weaken the bonding properties of certain materials (1,2,4,6–9). The thickness of MS layer depends on the blending time and the intensity of blending (10–12). Increased blending time with the lubricant present has a negative effect on the tablet hardness (3,13–16) and compactibility, especially with plastic materials (6) such as starches and microcrystalline cellulose (MCC). They are more prone to this negative effect of MS because they do not fragment during compression; thus, no new MS-free surfaces are available for bonding (3,4,7,16,17).

Bolhuis *et al.* (14) stated that when operating at the same rotation speed, the decrease in crushing strength was much faster in larger scale blenders than when using small-scale laboratory blenders. This is due to the higher shear forces in the former, resulting in faster film formation (14,18–20). The increase in the blender volume is also known to affect the kinetics of the lubrication process itself (21).

Segregation can also pose a problem during the tableting process (22,23). It is known to be more pronounced with larger particles such as granules and when the size distribution is broad. Even if the size difference between MS and MCC particles is typically significant, segregation is not usually a problem mainly because the mixture of MS and MCC is an ordered (or cohesive) mixture as MS covers the MCC particles (13). In the cohesive mixture, the movement of single particles is prevented by the relatively strong forces between the particles.

There have been numerous attempts to detect lubricant films by chemical or physical methods in order to get better understanding of the nature of these films. However, most of these investigations have relied on indirect techniques (24). Energy-dispersive X-ray microanalysis (EDX) has been applied to detect MS from surfaces. Pintye-Hódi *et al.* (25) succeeded to detect the magnesium peak at higher amounts

[1] Division of Pharmaceutical Technology, Faculty of Pharmacy, University of Helsinki, Viikinkaari 5E, P.O. Box 56, 00014 Helsinki, Finland.
[2] Department of Organic Chemistry and Technology, Budapest University of Technology and Economics, 8 Budafoki str., 1111 Budapest, Hungary.
[3] Orion Corporation, Orion Pharma, Orionintie 1, P.O. Box 65, 02101 Espoo, Finland.
[4] To whom correspondence should be addressed. (e-mail: satu.lakio@helsinki.fi)

of MS. The thickness of the film was found to be variable and even after 1 h blending time MS crystals were found in the blend. It is also postulated that MS can enter cavities in the excipients (26). In addition, Hussain *et al.* (27) estimated of the surface coverage by EDX. Abe and Otsuka (28) used electron probe microanalyzer to characterize MS coverage on potato starch particles. They found a difference in coverage after 0 and 180 min blending time. Secondary ion mass spectrometry has been used to detect MS as well (29,30). It seemed that the lubricant film is a blotchy rather than a continuous layer (29), and it forms in minutes (30). In addition, flame atomic absorption spectroscopy method has been used to evaluate MS distribution (31). Levels of MS as low as 0.05% has been detected by near-infrared spectroscopy (NIRS) from powder blends (32). NIRS has also been used to monitor MS blending process and its effect on prolonged dissolution time (28). NIRS and laser-induced breakdown spectroscopy have each been demonstrated to be capable of rapid MS analysis in the range of 0.1–2% most typically encountered in pharmaceutical powders and solid dosage forms (33).

The use of chemical imaging based on vibrational spectroscopy (infrared, near infrared, and Raman) has been rapidly increasing in the field of pharmaceutical technology during past few years. Raman imaging is a non-destructive method, and it gives information about the chemical composition, structure, and morphology of solid pharmaceuticals. The spatial distribution of components in tablets has been analyzed using Raman imaging and mapping (34–42).

Raman mapping can be a very slow process depending on the equipment and the chosen parameters. However, new equipment and measuring methods are making the process faster. This method can be used, for example, to measure the uniformity of blending, the existence of agglomerates and the migration of material during aging. Raman spectroscopy enables the detection of MS on the surfaces of the tablets and powders. Raman directly measures hydrophobic CH_2 – groups in MS (43). Henson and Zhang (44) measured low-dose tablets using Raman mapping. According to their results, Raman mapping reveals information about the distributions of the drug and, roughly, even the particle size. They emphasize that, based on the images, it cannot be told if there is one large particle, agglomerate, or loose particles next to each other. Micro-Raman spectroscopy is a convenient method for surface analysis because it can provide specific chemical information with good spatial resolution. Appropriate selection of laser source and microscopic objective (magnification) can provide laser spot sizes of 1 μm diameter or smaller (45,46).

Vajna *et al.* (42) used Raman imaging for detecting structural differences in imipramine tablets. They found that the distribution of MS can be properly visualized using high spatial and optical resolution. The laser spot size and the sampled depth with the ×10 objective was too large to capture MS signals. However, using ×100 magnification, distinct particles of the lubricant were detected. Widjaja and Seah (47) detected low concentrations (0.2–2.0% *w*/*w*) of MS using Raman microscopy and band-target entropy minimization technique. MS has also been determined at concentration levels of 0.5% (*w*/*w*) from powders and 3% (*w*/*w*) from tablets (43). MS seemed to be located on the surface of particles (46). However, in another study, it seemed that no obvious spectral information of MS (2% *w*/*w*) existed in the image data when measuring tablet using Raman spectroscopy (39). It can be thus concluded that the determination of MS with Raman spectroscopy is formulation and set-up dependent.

The aim of the study was to characterize the distribution of MS in MCC tablets using Raman chemical imaging. Different blending times and scales were used to demonstrate the effect of MS on the crushing strength of the tablets. Crushing strength of tablets was chosen as a secondary response to (over)lubrication because the decrease in crushing strength is known to demonstrate the lubrication phenomenon well.

MATERIALS AND METHODS

Materials

The lubricant effect of magnesium stearate (MS) was studied on binary blends of MS (1% *w*/*w*) (Ph. Eur., Orion Pharma, Espoo, Finland) and microcrystalline cellulose (MCC) (99% *w*/*w*) (PH101, IMCD Sweden AB, Malmö, Sweden).

Methods

Scanning Electron Microscopy

A scanning electron microscopy (SEM) (Zeiss DSM 962, Oberkochen, Germany) was used to illustrate the particle size and shape. Powder was sprinkled on top of a carbon tape, and loose particles were removed with pressurized air. Samples were then coated with conductive platinum coating in vacuum evaporation coater. SEM micrographs were obtained at an acceleration voltage of 10 kV and magnification of ×500 was used. SEM images are presented in Fig. 1.

Blending and Tableting

The binary blends of MS and MCC were manufactured. The blend was loaded into a glass jar in a systematic fashion, with MS in the middle of the glass jar (49.5% MCC–1% MS–49.5% MCC). Three blending scales were used: laboratory (1 L), pilot (10 L), and production (80 L). In addition, two replicates were made from each scale. Laboratory and pilot scale were blended using laboratory drum blender (Medikalla Oy, Kuopio, Finland), and production scale was blended with production drum blender (Winkworth blender SDT 65, Staines, UK). The batch sizes were 400 g with 1 L container, 4,000 g with 10 L container, and 32,000 g with 80 L container. The filling rate was 67% (*v*/*v*) for every scale. Blending times were 1, 2, 3, 5, 10, 30, 60, and 90 min. All the other variables were kept constant: the blender type (drum blender), the

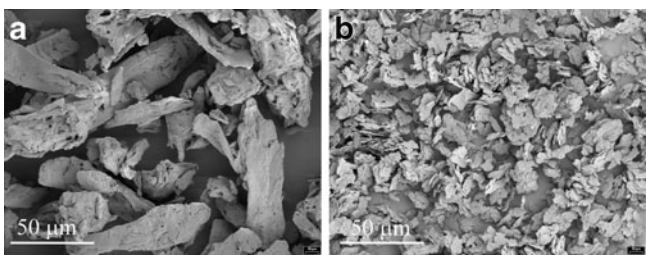

Fig. 1. SEM pictures of **a** MCC and **b** MS (magnification, ×500, scale bar 50 μm in the figures)

powder loading to the container, and the rate of rotation (12 rpm). The powder masses were allowed to adjust in a constant humidity of 50% ±2% RH for 2 weeks before tableting. The blends were tableted with eccentric tablet press (Hanseaten E1, Wilhelm Fette GmbH, Schwarzenbek, Germany) using flat 9-mm punches. The weight of the tablets was adjusted to 250 mg. The tablets were individually weighed before the Raman measurements. In addition, the crushing strengths of three tablets were measured using diametral hardness tester (Dr. K. Schleuniger & Co. 2 E, Thun, Switzerland) from each blending time point.

Raman Mapping Set-Up

Raman mapping spectra were collected on a Horiba Jobin-Yvon LabRAM system (Lyon, France) coupled with an external 532 nm Nd–YAG laser source and an Olympus BX-40 optical microscope. A high magnification objective (×100) was used for optical imaging and spectra acquisition. When acquiring a spectrum, the laser beam is directed through the objective, and backscattered radiation is collected with the same objective. The collected radiation is directed through a notch filter that removes the Rayleigh photons, then through a confocal hole and the entrance slit onto a grating monochromator (1,800 grooves/mm) that dispersed the light before a charge-coupled device detector. Spectral resolution was approximately 3 cm^{-1}. Exposition time was 2 s and spectra were averaged 10 times at each point. The measured spectral range was 182–1,652 cm^{-1}, but only the range of 870–1,652 cm^{-1} was chosen for modeling the data. Spatial step size was 5×5 μm, and the measured area was 49×49 points (pixels), covering an area of 250×250 μm.

Raman Mapping of Tablets

Raman maps were collected from the surface of the tablets. All spectra were baseline corrected to remove the fluorescent background using piecewise linear baseline correction with the same baseline points for all the maps and reference spectra. The Raman spectra of all points were modeled with classical least squares (CLS) method using the pure component spectra of MCC and MS. The method is described in details by Vajna *et al.* (42). The modeling gives a spectral score (that is in correlation with the concentration) for all the components. The score ranges from 0 to 1, where 0 means that the ingredient is not present (or is under limit of detection) in the measured area, while 1 means that the point consists of that component only. Distribution maps of the MS were created by plotting the CLS spectral scores against the *X* and *Y* spatial coordinates. Several different statistical parameters were calculated to describe the differences among the samples, such as average, standard deviation, maximum observed score, skewness, kurtosis, and median. Mean and median indicate the average spectral MS content in the tablets, while the other parameters help to assess the heterogeneity of the MS. The spectral concentrations are not equal to the real (*e.g.*, mass percent) concentrations, but have been shown to be good approximations for real concentrations (36,42). Raman mapping was performed on tablets made from blends at blending times of 2, 5, 30, and 60 min.

Data Analysis

The comparison of Raman maps was carried out both visually and statistically. The visualized concentration maps give information about the spatial distribution. The color scale (0–0.73) assigned to the concentrations was chosen to yield the most clearly visible and comparable pictures. Additionally, a histogram was calculated for each Raman map, describing the mathematical distribution of the calculated concentrations. The histograms were produced using MATLAB 7.10 (MathWorks, Natick, MA, USA) and Excel 2007 (Microsoft Corp., Redmond, WA, USA).

Student's *t* test at 95% confidence level (paired media) was applied to compare the differences between blending scales. Individual time points were compared between different blending scales.

RESULTS

The Effect of Magnesium Stearate on Crushing Strength of Tablets

The crushing strength of tablets was generally found to decrease with the increase of blending time (Fig. 2). The *Y*-axis in Fig. 2 is presented as the crushing strength of tablets divided by their individual weight (48). This operation made the values better comparable. Logarithmic trend line was fitted to the data because the crushing strength of the tablets is known to decrease, when the blending time increases, in a semilogarithmic manner (18). The decrease in crushing strength was more pronounced in larger production scales. The difference was not substantial during the first few minutes, although the 1-L scale could be already differentiated from larger scales. The difference between scales was more apparent after 3 min.

The differences between 10 and 80 L were smaller than between 1 L and larger scales. Statistical Student's *t* test at 95% confidence level was applied to compare the differences among blending scales. The resulting *p* values indicated that there was statistically significant difference, at every time point, between the time points of 1- and 10-L scale and between 1- and 80-L scale ($p<0.05$). Statistically significant difference between the time points of 10- and 80-L scale was achieved only at longer blending times, from 5 min onwards ($p<0.05$). The results suggest that lubrication was more efficient in larger scales. Even if the filling rate was the same in all of the scales, the effect of the container walls could be different. MS could not disappear during the blending process, but it was possible that the MS particles adsorbed onto container walls, to give the impression that there was less MS in the mass. Hence, using a smaller container resulted in relatively more effective MS adsorption to the container walls due to the higher ratio of wall area and container volume. Therefore, MS stayed more efficiently within the bulk powder at larger scales, resulting in a higher amount of MS being present in the final tablets. In addition, there was higher number of individual particles in the larger scale containers, which affected on the blending phenomenon itself. Thus, 80-L batches should have more significant reduction in the crushing strength than 10-L batches. In addition to the phenomena above, MS could also be adsorbed onto the punches and the die walls during the

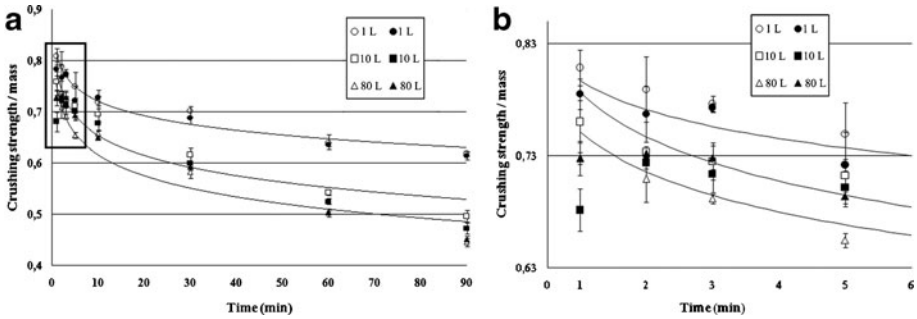

Fig. 2. The crushing strength of tablets decreased when the blending time increased. **a** Time points from 1 min to 90 min. **b** Time points from 1 min to 5 min (*black box* from **a**)

tableting process. This could lead to a higher concentration of MS on the surfaces of the tablets. However, the decrease in crushing strength was mainly due to the MS coating.

As mentioned earlier, the crushing strength of tablets decreased as the blending time increased. This was concluded to result from the coating of MCC by MS during blending. During the MS blending, the free MS particles are at first adsorbed on the surfaces of the excipient and drug particles, and then, they shear off the agglomerates and become distributed evenly on the surfaces (3). Hence, the crushing strength of tablets could be used as a reference for the lubrication effect and the tablets could be used for Raman spectroscopy measurements.

Raman Mapping

Uniformity of tablet surfaces was ensured in preliminary Raman mapping by collecting spectra from various areas throughout tablet surfaces (results not shown). Raman maps were measured from tablets of every blending scale (1, 10, and 80 L). Time points were selected to be 2, 5, 30, and 60 min. The first time point (1 min) was not used for mapping because such short duration of blending results in a high degree of both between- and within-tablet heterogeneities. Thus, altogether 12 tablets were measured. The spectra measured from the pure MS and MCC and spectrum measured from tablet are presented in Fig. 3.

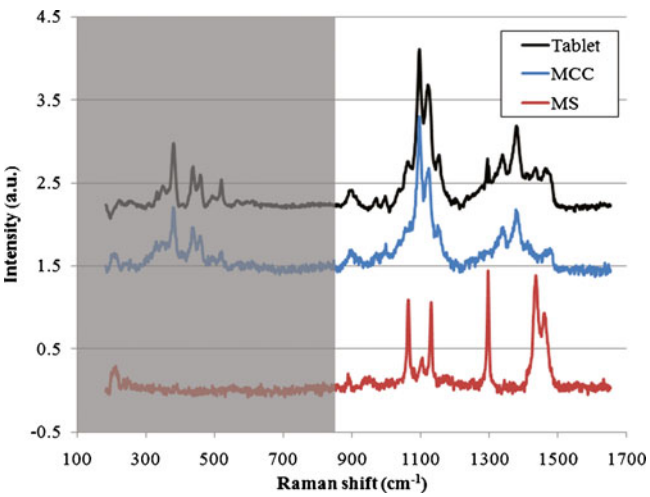

Fig. 3. Raw Raman spectrum measured from the MS (*red*), MCC (*blue*), and the example tablet (*black*). The range (870–1,652 cm^{-1}) on the white background was chosen for data analysis

The Raman maps in Figs. 4, 5, and 6 give information about the spatial distribution of MS within the investigated tablets. The same color scale (0–0.73) was used to achieve comparable pictures. High spectral concentration (also known as Raman score, which is in correspondence with the true concentration) for MS is shown with lighter colors, while darker colors correspond to high concentration of MCC. Additionally, histograms were calculated for the scores observed in each Raman map, describing the mathematical distribution of the calculated concentrations (Figs. 4, 5, and 6). For clarity, the highest bars (more than 400 pixels) are cut off in the histograms. In such cases, the number of pixels is numerically indicated above the bar. The last bar in each histogram represents all MS concentration values over 15%.

The distribution of MS in the tablet which mass was homogenized for 2 min is shown in Fig. 4a. There were areas that contained MS in very high concentration (yellow points on the image). In the histogram (Fig. 4b), this was represented by the fact that the number of pixels with more than 15% MS was very high. Furthermore, it could be observed that there were numerous MS aggregates on the image. The histogram showed that there were also a lot of pixels, which contained no MS at all (Fig. 4b). There were still large MS particles in the sample prepared after 5 min blending (Fig. 4c). It could be seen, however, that the number of pixels containing ~3–9% MS was higher in the 5 min than in the 2 min sample (Fig. 4d). This also suggested that MS started to form a layer on the MCC particles. In addition, there was less yellow color in the figure indicating the disintegration of MS aggregates, corresponding to a lower maximum MS concentration within the entire Raman map. After 30 min blending, there were less large particles of MS than in the sample homogenized for 5 min. In addition, there were no particles with very high concentrations of MS. The histogram shows the increasing number of pixels containing low concentration of MS (Fig. 4f). Furthermore, the last bar representing MS values over 15% is really low. Figure 4g showed blurred and almost disintegrated particles of MS on the whole surface after 60 min of blending. However, few MS clusters could still be detected.

When investigating 10-L scale, large MS clusters could be identified in the tablet homogenized for 2 min (Fig. 5a). The histogram showed that there also were plenty of pixels with no MS at all. There were still large particles of MS in the sample after 5 min blending (Fig. 5c). However, the clusters had started to spread, which indicated that MS had started to form a layer on the MCC particles. After 30 min blending, the clusters became smaller (Fig. 5e), and there were less large

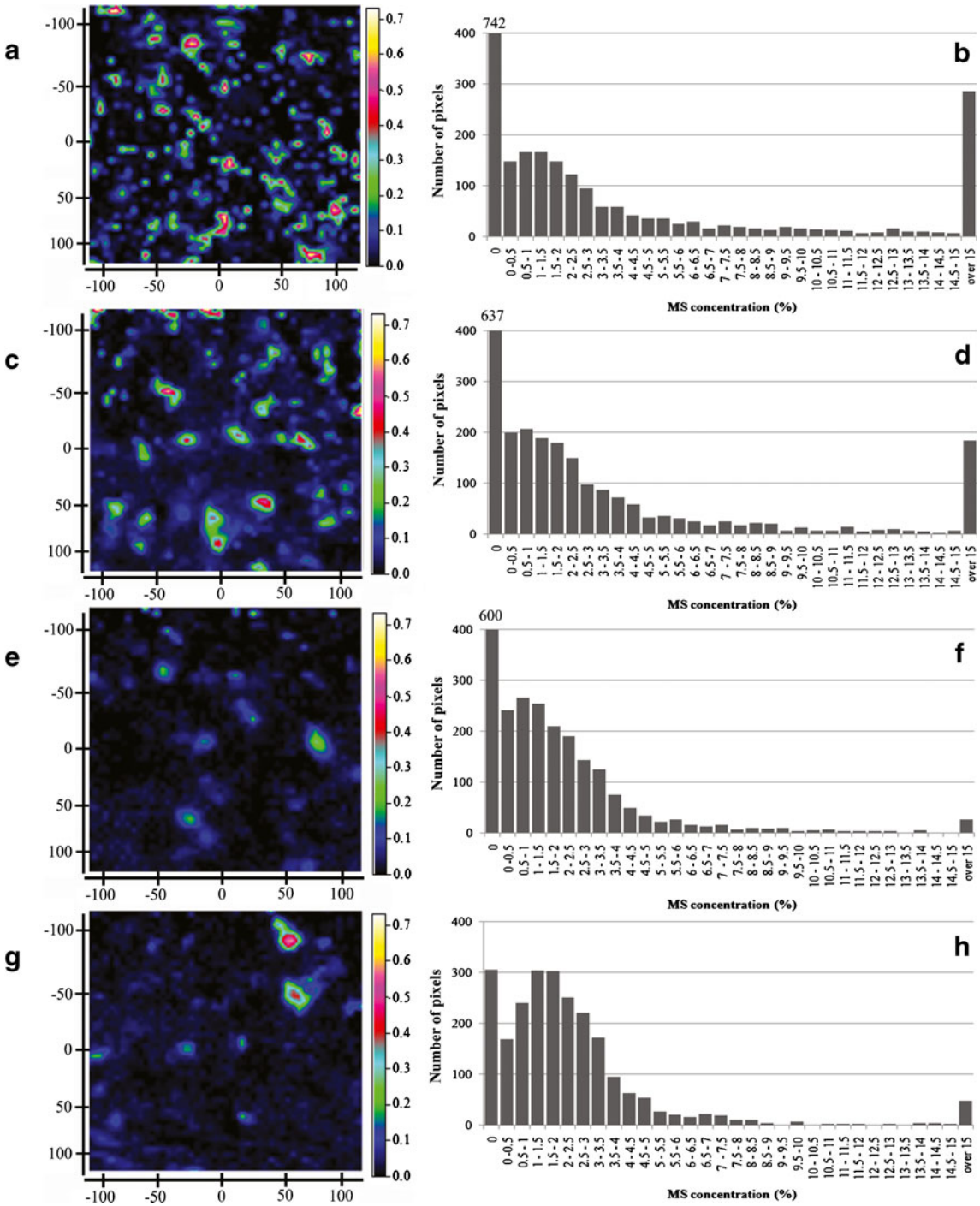

Fig. 4. The distribution of MS on the tablets and corresponding histograms. Blending scale 1 L. Blending time: **a** 2 min, **b** 2 min histogram, **c** 5 min, **d** 5 min histogram, **e** 30 min, **f** 30 min histogram, **g** 60 min, and **h** 60 min histogram. The *last bar in the histograms* represents pixels that contained more than 15% of MS. The first bars are cut-off due to high values; corresponding values are marked over the bars

particles of MS than in the sample homogenized for 5 min. In addition, there were fewer particles with very high concentrations of MS. Figure 5g showed blurred and almost disintegrated particles of MS on the whole surface after 60 min of blending. It seemed that MS particles have widely coated MCC particles.

Visually, it seemed that the Raman maps after 2 and 5 min blending were quite similar (Fig. 6a). However, difference can be observed by reviewing the histograms. The amount of pixels containing 0.5–4% of MS was higher after 2 min blending, suggesting that, in this case, MS was not spread more efficiently after 5 min blending. Interestingly, after 30 min blending, there were still MS clusters (Fig. 6e). After 60 min of blending, the clusters have disintegrated and MS has spread quite evenly on the tablet surface, which can be observed as bluish

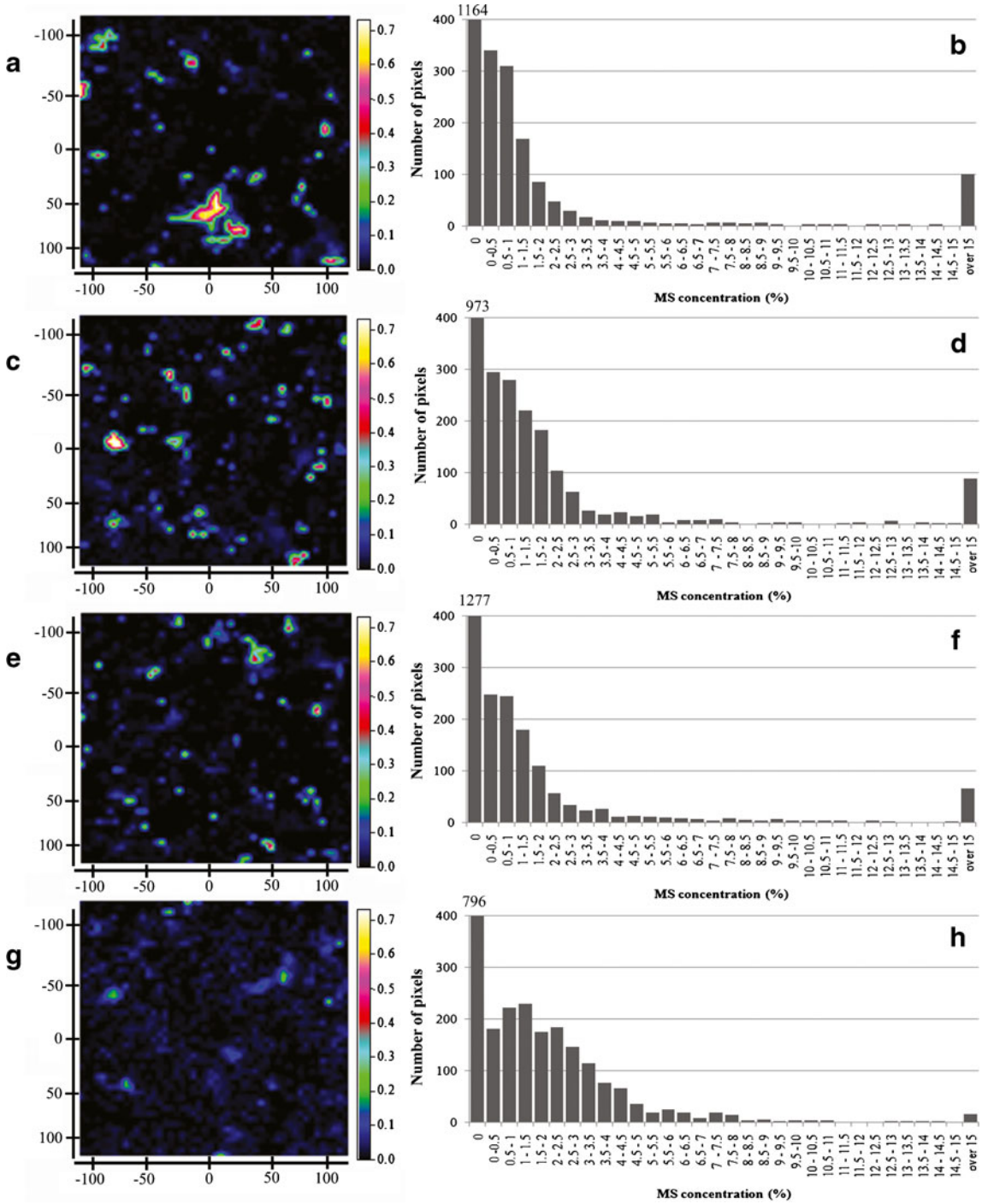

Fig. 5. The distribution of MS on the tablets and corresponding histograms. Blending scale 10 L. Blending time: **a** 2 min, **b** 2 min histogram, **c** 5 min, **d** 5 min histogram, **e** 30 min, **f** 30 min histogram, **g** 60 min, and **h** 60 min histogram. The *last bar in the histograms* represents pixels that contained more than 15% of MS. The first bars are cut-off due to high values; corresponding values are marked over the bars

background and high amount of pixels containing MS around 2–5% in the histogram (Fig. 6h).

When inspecting the 2 min time point for every scale, it was noticed that the blending effect was more pronounced when going towards larger scales. While local deviations exist from the general trends, it can be concluded that the homogenization of MS blending occurs faster at larger scales, as also seen on the slope of trending curves on Fig. 2.

Statistical Parameters

Descriptive statistics concerning Raman maps are shown in Table I, which gives further information about the blending processes. For instance, when comparing time points between different scales, the skewness and kurtosis values were larger with 10- and 80-L scales than with 1-L scale. In addition, the average and the relative

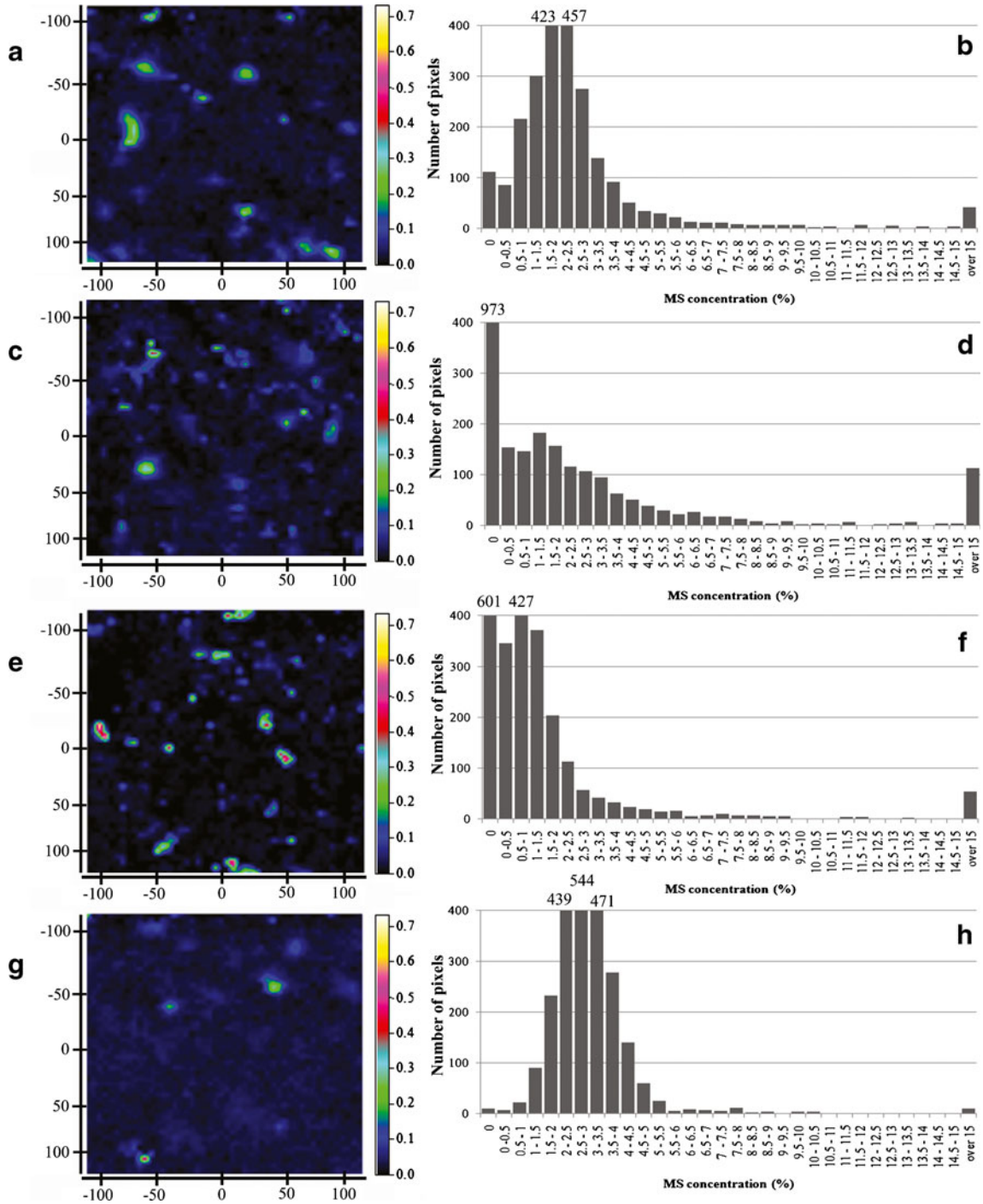

Fig. 6. The distribution maps of MS on the tablets and corresponding histograms. Blending scale 80 L. Blending time: **a** 2 min, **b** 2 min histogram, **c** 5 min, **d** 5 min histogram, **e** 30 min, **f** 30 min histogram, **g** 60 min, and **h** 60 min histogram. The last bar in the histograms represents pixels that contained more than 15% of MS. The first bars are cut-off due to high values; corresponding values are marked over the bars

standard deviation decreased when the blending time increased. In theory, the maximum values and standard deviation of Raman scores (spectral concentrations in the separate pixels) should decrease as the homogeneity increases. References towards this can be observed in Table I. However, how relevant these trends are is unknown. The drawback of the abovementioned statistical values is that these descriptive parameters (except the median) are mostly valid only if the distribution of score values is close to Gaussian. This is, to the authors' experience, not the usual case with Raman maps. The distributions beside the histograms in the previous section can be also illustrated with box plots (Fig. 7) showing the median, the range of the closest ±25% of points to the median, along with the non-outlier range and the outliers. The statistical parameters support the general observations, but the main

Table I. Descriptive Statistics of Raman Mapping Results

Parameter	Scale (L)	2 min	5 min	30 min	60 min
Average	1	0.059	0.043	0.020	0.027
	10	0.025	0.024	0.017	0.018
	80	0.027	0.029	0.058	0.031
St dev	1	0.18	0.085	0.031	0.045
	10	0.088	0.080	0.055	0.028
	80	0.034	0.067	0.054	0.011
Rel st dev	1	1.98	1.98	1.52	1.69
	10	3.57	3.36	3.32	1.56
	80	1.23	2.31	0.92	0.35
Median	1	0.014	0.014	0.012	0.018
	10	0.001	0.004	0.000	0.010
	80	0.021	0.008	0.008	0.029
Max	1	0.790	0.72	0.37	0.61
	10	0.96	1.00	0.76	0.44
	80	0.47	0.58	0.84	0.58
Skewness[a]	1	1.52	1.50	1.49	1.41
	10	2.97	2.21	2.50	1.36
	80	2.02	1.34	2.38	2.12
Kurtosis[a]	1	0.87	0.83	0.74	0.50
	10	8.18	3.74	5.28	0.33
	80	3.15	0.41	4.55	3.45

The parameters have been calculated using pixel information of ms distribution in raman maps
St dev standard deviation, *Rel st dev* relative standard deviation, *Max* maximum value
[a] Without the first and the last bar in the histogram

sources of information are the Raman score maps themselves because they give visual information about the progress of the blending process.

DISCUSSION

Usually, the aim of the blending process is to achieve homogeneity. However, MS blending differs quite dramatically from any other blending scenarios. The lubricant needs to be distributed within the mass sufficiently to allow efficient and problem-free tableting. Simultaneously, MS particles start coating particles of other materials and thus prohibit the bonding between particles. If the optimal blending time is exceeded, overlubrication happens. This overlubrication is also called *the magnesium stearate effect*. Although overlubrication of powder mass during MS blending is a well-known problem, the lubricant distribution in tablets has been traditionally challenging to measure. There is currently no adequate analytical method to detect this phenomenon precisely and fast.

Raman spectroscopy can be utilized for measuring the lubrication effect of MS. Raman mapping can differentiate 2 min blending from 60 min blending, but it remains to be seen if 2 min blending from 5 min blending can be differentiated in a statistically significant manner, which would be more useful when considering real-life needs. In order to increase the sensitivity of the statistical evaluation, a great number of samples are required. More work is needed on that field.

The MS percentages calculated with CLS method based on the Raman spectra were a bit higher than the real MS concentrations. However, it has been stated that the Raman scores are only approximating the real concentrations (42) and results

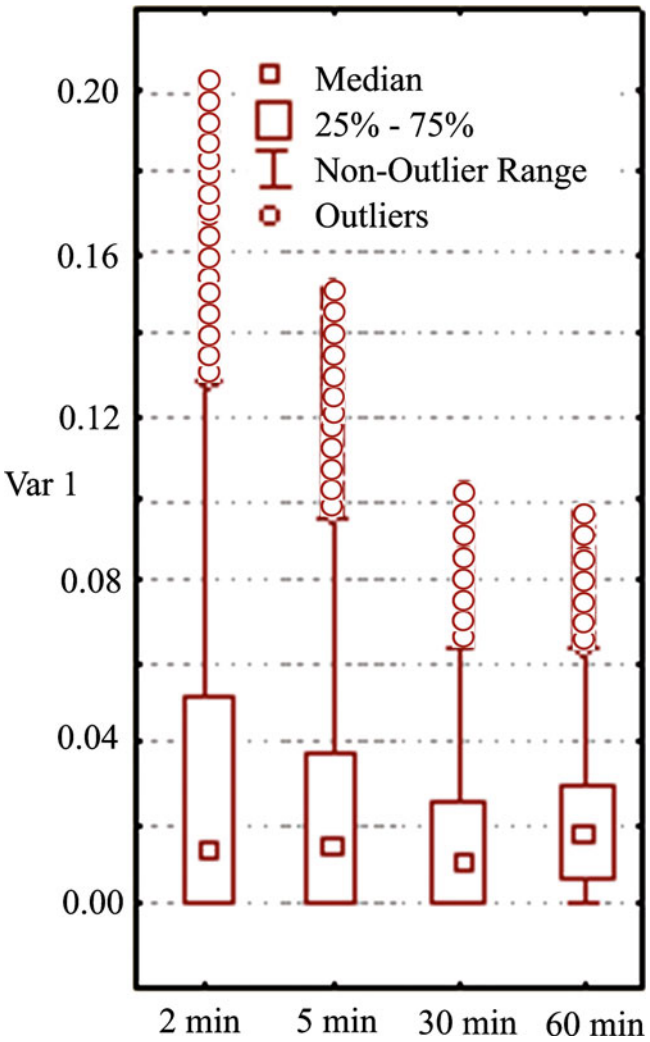

Fig. 7. The MS distributions illustrated with box plots for 1-L scale showing the median (*square*), the range of the closest ±25% of points to the median (*rectangle*), the non-outlier range (*line*), and the outliers (*circle dots*)

serve only a semiquantitative approach, and it is more reliable to compare trends than actual MS concentrations.

The measured area was 250×250 μm, and the step size was 5 μm for the Raman mapping. The particle size of MS was around 10 μm. Thus, it is safe to assume that Raman is able to observe most of the MS particles. However, some MS particles can be sheared during blending and tableting and the particle size can be decreased under the detection limit, which was 1% (±0.5%) per pixel. As MS gets homogenized, some pixels may contain MS below the detection limit and may result in the overall loss of average MS score. The coating of the larger particles with smaller particles is generally considered a challenging task for spectroscopic measurements (49).

In addition to the already mentioned considerations, there are plenty of other parameters to be considered when collecting Raman maps, with the integration time, step size, measured area, used wavelength, and laser power being the most important issues. When the integration time is increased, step size decreased, wavelength range increased, or area increased the measuring time increases. Thus, the time is the limiting factor in these kinds of measurements. In this study, increasing the measured area was not a priority as the primary

concern was the high magnification to ensure appropriate detection of MS particles. Thus, MS can be qualitatively detected from the tablet surface, but quantitative determination would demand massive amount of repetitive measurements that would be too laborious and time-consuming with the point mapping set-up. However, the results are still suggestive and highly informative and reveal new insights to MS blending. In addition, they demonstrate the potential of Raman mapping in this kind of study.

CONCLUSIONS

Monitoring of MS blending is an extremely challenging and difficult process due to the low overall concentration of the lubricant and the fact that the phenomenon of interest is not directly linked with any chemical properties of the mass.

The aim of this study was to investigate the distribution of MS in MCC tablets in three different blending scales. The crushing strength of tablets against the blending time behaved similarly for all the production scales. MS blending was found to be more efficient in larger scales. However, the results gained from the laboratory scale could not directly predict the blending time for greater scales without altering the crushing strength of tablets in the scaling-up process.

In addition, coating of the MCC particles with MS particles in intact tablets was detected using imaging Raman spectroscopy. The Raman method is non-invasive and can provide highly valuable visual information about the progress of the blending process, and it can be used to detect MS in MCC tablets. However, the process is time-consuming and demands precision.

ACKNOWLEDGMENTS

The authors would like to thank Anna Shevchenko and Dr Simo Siiriä for their contribution during the study.

REFERENCES

1. Strickland WA, Nelson E, Busse LW, Higuchi T. The physics of tablet compression. IX. Fundamental aspects of tablet lubrication. J Am Pharm Assoc. 1956;45(1):51–5.
2. Vitková M, Chalabala M. The use of some hydrophobic substances in tablet technology. Acta Pharm Hung. 1998;68 (6):336–44.
3. Bolhuis GK, Lerk CF, Zijlstra HT, De Boer AH. Film formations by magnesium stearate during mixing and its effect on tableting. Pharm Weekblad. 1975;110(16):317–25.
4. de Boer AH, Bolhuis GK, Lerk CF. Bonding characteristics by scanning electron microscopy of powders mixed with magnesium stearate. Powder Technol. 1978;20(1):75–82.
5. Ragnarson G, Hölzer AW, Sjögren J. The influence of mixing time and colloidal silica on the lubricating properties of magnesium stearate. Int J Pharm. 1979;3(2–3):127–31.
6. Vromans H, Lerk CF. Densification properties and compactibility of mixtures of pharmaceutical excipients with and without magnesium stearate. Int J Pharm. 1988;46(3):183–92.
7. Zuurman K, Van der Voort Maarschalk K, Bolhuis GK. Effect of magnesium stearate on bonding and porosity expansion of tablets produced from materials with different consolidation properties. Int J Pharm. 1999;179:107–15.
8. Jarosz PJ, Parrott EL. Effect of lubricants on tensile strength of tablets. Drug Dev Ind Pharm. 1984;10(2):259–73.
9. Faqih AMN, Mehrotha A, Hammond SV, Muzzio FJ. Effect of moisture and magnesium stearate comcentration on flow properties of cohesive granular materials. Int J Pharm. 2007;336:338–45.
10. Lerk CF, Bolhuis GK, Smedema SS. Interactions of lubricants and colloidal silica during mixing with excipients I. Its effect on tableting. Pharm Acta Helv. 1977;52(3):33–9.
11. Shah AC, Mlodozeniec AR. Mechanism of surface lubrication: Influence of duration of lubricant-excipient mixing on processing characteristics of powders and properties of compressed tablets. J Pharm Sci. 1977;66(10):1377–82.
12. Johansson ME, Nicklasson M. Investigation of the film formation of magnesium stearate by applying a flow-through dissolution technique. J Pharm Pharmacol. 1986;38:51–4.
13. Bolhuis GK, Lerk CF. Ordered mixing with lubricant and glidant in tableting mixtures. J Pharm Pharmacol. 1981;33(12):790.
14. Bolhuis GK, de Jong SW, Lerk CF, Dettmers H. The effect of magnesium stearate admixing in different types of laboratory and industrial mixers on tablet crushing strength. Drug Dev Ind Pharm. 1987;13(9–11):1547–67.
15. van der Watt JG. The effect of the particle size of microcrystalline cellulose on tablet properties in mixtures with magnesium stearate. Int J Pharm. 1987;36:51–4.
16. Kikuta JI, Kitamori N. Effect of mixing time on the lubricating properties of magnesium stearate and the final characteristics of the compressed tablets. Drug Dev Ind Pharm. 1994;20(3):343–55.
17. Mollan Jr MJ, Çelik M. The effects of lubrication on the compaction and post-compaction properties of directly compressible maltodextrins. Int J Pharm. 1996;144(1):1–9.
18. Malmqvist K, Nyström C. Studies on direct compression of tablets IX: the effect of scaling-up on the preparation of ordered mixtures in double-cone mixers. Acta Pharm Suec. 1984;21 (1):21–30.
19. Johansson ME. The effect of scaling-up of the mixing process on the lubricating effect of powdered and granular magnesium stearate. Acta Pharm Technol. 1986;32(1):39–42.
20. Kushner J, Moore F. Scale-up model describing the impact of lubrication on tablet tensile strength. Int J Pharm. 2010;399:19–30.
21. van der Watt JG, de Villier MM. The effect of V-mixer scale-up on the mixing of magnesium stearate with direct compression microcrystalline cellulose. Eur J Pharm Biopharm. 1997;43:91–4.
22. Lakio S, Siiriä S, Räikkönea H, Airaksinen S, Närvänen T, Antikainen O, *et al*. New insights into segregation during tableting. Int J Pharm. 2010;397:19–26.
23. Lakio S, Hatara J, Tervakangas H, Sandler N. Determination of segregation tendency of granules using surface imaging. J Pharm Sci. 2012;101(6):2229–38.
24. Bolhuis GK, Hölzer AW. Lubrication issues in direct compaction. In: Çelik M, editor. Pharmaceutical Powder Compaction Technology. 2nd ed. Dublin: Informa Healthcare; 2011.
25. Pintye-Hódi K, Tóth I, Kata M. Investigation of the formation of magnesium stearate film by energy dispersive X-ray microanalysis. Pharm Acta Helv. 1981;56(11):320–4.
26. Roblot-Treubel L, Puisieux F. Distribution of magnesium stearate on the surfaces of lubricated particles. Int J Pharm. 1986;31(1–2):131–6.
27. Hussain MSH, York P, Timmins PA. Study of the formation of magnesium stearate film on sodium chloride using energy-dispersive X-ray analysis. Int J Pharm. 1988;42(1–3):89–95.
28. Abe H, Otsuka M. Effects of lubricant-mixing time on prolongation of dissolution time and its prediction by measuring near infrared spectra from tablets. Drug Dev Ind Pharm. 2012;38 (4):412–9.
29. Davies MC, Brown A, Newton JM. Chemical characterisation of lubricant films. J Pharm Pharmacol. 1987;39(Suppl):122P.
30. Hussain MSH, York P, Timmins P, Humphrey P. Secondary ion mass spectroscopy (SIMS) evaluation of magnesium stearate distributions and its effects on the physic-technical properties of sodium chloride tablets. Powder Technol. 1990;60 (1):39–45.
31. Sugisawa K, Kaneko T, Sago T, Sato T. Rapid quantitative analysis of magnesium stearate in pharmaceutical powders and solid dosage forms by atomic absorption: method development and application in product manufacturing. J Pharm Biomed Anal. 2009;49:858–61.

32. Duong NH, Arratia P, Muzzio F, Lange A, Timmermans J, Reynolds S. A homogeneity study using NIR spectroscopy: tracking magnesium stearate in Bohle Bin-blender. Drug Dev Ind Pharm. 2003;29(6):679–87.
33. Green RL, Mowery MD, Good JA, Higgins JP, Arrivo SM, McColough K, *et al*. Comparison of near-infrared and laser-induced breakdown spectroscopy for determination of magnesium stearate in pharmaceutical powders and solid dosage forms. Appl Spectrosc. 2005;59(3):340–7.
34. Bell SEJ, Barett LJ, Burns DT, Dennis AC, Speers SJ. Tracking the distribution of "ecstasy" tablets by Raman composition profiling: A large scale feasibility study. Analyst (Cambridge UK). 2004;128:1331–5.
35. De Juan A, Tauler R, Dyson R, Marcolli C, Rault M, Maeder M. Spectroscopic imaging and chemometrics: a powerful combination for global and local sample analysis. Trends Anal Chem. 2004;23(1):70–9.
36. Šašić S, Clark DA, Mitchell JC, Snowden MJ. A comparison of Raman chemical images produced by univariate and multivariate data processing—a simulation with an example from pharmaceutical practice. Analyst (Cambridge UK). 2004;129:1001–7.
37. Šašić S, Morimoto M, Otsuka M, Ozaki Y. Two-dimensional correlation spectroscopy as a tool for analyzing vibrational images. Vib Spectrosc. 2005;37:217–24.
38. Šašić S, Clark DA, Mitchell JC, Snowden MJ. Analyzing Raman maps of pharmaceutical products by sample–sample two-dimensional correlation. Appl Spectrosc. 2005;59:630–8.
39. Zhang L, Henson M, Sekulic SS. Multivariate data analysis for Raman imaging of a model pharmaceutical tablet. Anal Chim Acta. 2005;545:262–78.
40. Clark D, Šašić S. Chemical images: technical approaches and issues. Cytometry. 2006;69:815–24.
41. Šašić S. An in-dept analysis of Raman and near-infrared chemical images of common pharmaceutical tablets. Appl Spectrosc. 2007;61(3):239–50.
42. Vajna B, Farkas I, Szabo A, Zsigmond Z, Marosi G. Raman microscopic evaluation of technology dependent structural differences in tablets containing imipramine model drug. J Pharm Biomed Anal. 2010;51:30–8.
43. Aquirre-Mendez C, Romanach RJ. A Raman spectroscopic method to monitor magnesium stearare in blends and tablets. Pharm Technol Europe. 1 September 2007. http://www.pharmtech.com/pharmtech//article/articleDetail.jsp?id=456225 Accessed 16 Jan 2012.
44. Henson MJ, Zhang L. Drug characterization in low dosage pharmaceutical tablets using Raman microscopic mapping. Appl Spectrosc. 2006;60(11):1247–55.
45. Malecha M, Bessant C, Saini S. Principal components analysis for the visualization of multidimensional chemical data acquired by scanning Raman microspectroscopy. Analyst. 2002;127(9):1261–6.
46. Clarke FC, Whitley A, Mamedov S, Adar F, Lewis N, Lee E. Raman and EDXRF chemical imaging for formulation process development and quality control. Spectroscopy—Solutions for material analysis, 2005 June. http://www.horiba.com/fileadmin/uploads/Scientific/Documents/Raman/SPJune2005.pdf Accessed 16 Jan 2012.
47. Widjaja E, Seah RKH. Application of Raman microscopy and band-target entropy minimization to identify minor components in model pharmaceutical tablets. J Pharm Biomed Anal. 2008;46:274–81.
48. De Jong JAH. Relations between tablet properties. Pharm Weekblad. 1987;9(1):24–8.
49. Virtanen S, Antikainen O, Yliruusi J. Uniformity of poorly miscible powders determined by near infrared spectroscopy. Int J Pharm. 2007;345(1–2):108–15.